# Euler Solutions of Transonic Vortex Flows Around the Dillner Wing

Arthur Rizzi*
*The Aeronautical Research Institute of Sweden, FFA, Bromma, Sweden*

**Two sets of solutions for a sharped-edged, nonconical, 70-deg swept delta wing in both subsonic and supersonic flight at 15-deg angle of attack are presented. The first is computed on a standard mesh of $65\times21\times29$ grid points, and the second on a denser mesh of up to $193\times57\times97$ points (over one million). The comparison of these two sets shows that as the mesh is refined the vorticity field becomes sharper, the suctions peaks higher, new shock phenomena appear, and the observed total pressure losses become more comprehensible.**

## Introduction

THE recent discovery that a vortex sheet can be created and captured in the numerical solution of the Euler equations for the simulation of a flowfield which separates from the leading edge of a delta wing at high angle of attack has stirred the imagination of the aeronautical community. (See Ref. 1 for a very good survey of the current state-of-the-art on modeling such flowfields numerically.) The practical uses of this simulation technique are many. Unlike its one competing method for this application—the panel method that incorporates a vortex-sheet model into a linear potential flowfield—only the Euler-equation approach is suited to the analysis of nonlinear transonic flowfields. It also holds the promise of being adapted to more general aircraft configurations. The initial euphoria surrounding this finding stems from the qualitatively realistic character of the numerical simulations—a vorticity field above the wing is obtained and is fed by a smeared sheet separating from the leading edge of the wing. However, to evaluate these results more critically is difficult, in part because our understanding of the physics of these flows in general, and for transonic ones in particular, is still incomplete, and in part because these are the first inviscid shed-vortex-flow solutions to be obtained.

Assessment of the realism of the computed flows lacks a good measure or control on the strength of the shed-vortex sheet. Some limited experimental pressure measurements show that the primary vortex is computed reasonably well, but secondary-vortex effects in the measurements cloud the issue. One way to gain insight, and perhaps the only alternative at present, is to compare, for a specific flow, the solutions given by various methods with the highest mesh resolution possible. Working Group 07 of AGARD has proposed two test cases, representative of shed-vortex flow, for the assessment of computed results. A number of solutions, including the present ones, have been carried out. While the comparison[2] does show some definite trends, other trends are inconclusive because the solutions were obtained with different methods using different mesh types of relatively coarse density (50,000 points or less). This paper outlines a method to solve the Euler equations. Solutions are presented for the AGARD Dillner wing test cases using the standard mesh of $65\times21\times29$ nodes. The results are compared with new results recently obtained on the CYBER 205 with 16 M words of memory using the same method and mesh type but with up to $193\times57\times97$ nodes. Some new flow features are revealed, in particular, the interaction of shock waves and vortices, and new conclusions are drawn about the overall quality of the numerical simulations.

Presented as Paper 84-2142 at the AIAA 2nd Applied Aerodynamics Conference, Seattle, Wash., Aug. 21-23, 1984. Received Oct. 26, 1984; revision received Jan. 4, 1985. 

*Research Scientist, Aerodynamics Department; also, Adjunct Professor of Computational Fluid Dynamics, Royal Institute of Technology, Stockholm, Sweden. Member AIAA.

## Numerical Method

The present solutions were produced with an explicit multistage, time-stepping, finite-volume method[3,4] that uses central differences to solve the Euler equations in the form

$$\frac{\partial}{\partial t}\int q\,\mathrm{dvol} = -\iint \boldsymbol{H}\cdot\boldsymbol{n}\,ds + \text{boundary conditions and artificial viscosity}$$

A new improvement is a refinement in the model for artificial viscosity (termed operator $Dq$). Setting the correct boundary conditions for the model is among the most troublesome and difficult aspects of the entire method. With insight from the computer-aided analysis of the convergence of the Euler equations to steady state, Eriksson[5] came upon a useful guideline, a quadratic property of $D$, for determining the boundary conditions; namely, that its quadratic form should be negative semidefinite ($q^TDq\le 0$. Skewed differences at the boundaries can then be derived so that this property is realized.[6] The computer program[7] itself is made up entirely of vector operations over a three-dimensional subset (whose size is chosen freely on input) of the total data structure, and repeats these operations in a "do loop" for each successive subset until the entire data set is processed, a programming technique commonly called "strip mining." In this way vector lengths between 40,000 and 60,000 are obtained easily for any given mesh dimension. The program executes with 32-bit precision at an average rate of about 125 M flops sustained over the entire computation.

## O-O Mesh Around Dillner Wing

The program computes solutions upon meshes of type O-O having a three-pole system of singular lines.[8] The advantage of this mesh type is the focusing of points along all aerodynamic edges and at the apex of the wing. The meshes used for the two sets of solutions differ only in number of points, not in type or distribution functions. Figure 1 shows chordwise and spanwise details of the mesh with $193\times57\times97$ points.

## Computed Results

The dominant flow feature of the two AGARD test cases is the vortex over the upper surface of the so-called Dillner wing,

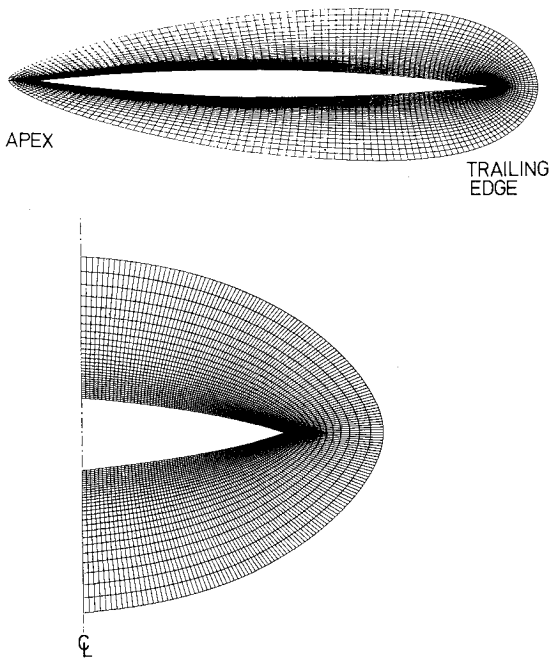


**Fig. 1 Partial chordwise and spanwise views of the 193×57×97 point O-O-type mesh around the Dillner wing.**

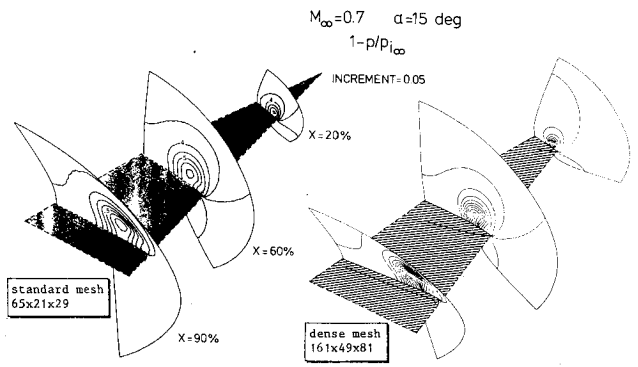


**Fig. 2 Comparison of standard- and dense-mesh solution isobars $1\text{-}p/p_{i_\infty}$ in three mesh surfaces at the 20, 60, and 90% chord stations of the Dillner wing. $M_\infty = 0.70$, $\alpha = 15$ deg.**

a 70-deg swept delta wing defined by spanwise sections of biconvex circular arc profiles whose maximum thickness (at midchord) is 6% of the local chord. At 15-deg incidence both the $M_\infty = 0.7$ and 1.5 cases contain mixed regions of subsonic and supersonic flow where the effects of vorticity and compressibility may interact strongly. The flow properties of interest are pressure (either $C_p$ or $1\text{-}p/p_{i_\infty}$ normalized by freestream total pressure $p_{i_\infty}$), Mach number, and the normalized loss in total pressure $1\text{-}p_i/p_{i_\infty}$, as well as the magnitude of vorticity $|\vec{\Omega}|$.

In order to give an overall impression of the computed flowfields over the wing, Fig. 2 presents three-dimensional isobars of the standard- and dense-mesh solutions in a side by side comparison. For both cases, subsonic and supersonic, with substantial mesh refinement there is no fundamental departure from a picture of vortex flow being fed by a shear layer shed from the leading edge of the wing, only sharper clearer features in the details of the flow. The position of the vortex remains virtually unchanged, and even the level of total pressure loss is about the same, only less diffuse. This verifies the validity of the Euler-equation model for this type of flow, and suggests that the creation of the vortex is insensitive to the grid resolution, at least for a sharp-edged wing.

The solution computed for the case of $M_\infty = 0.7$ and $\alpha = 15$ deg on a mesh of 160 cells around the semispan, 80 on the

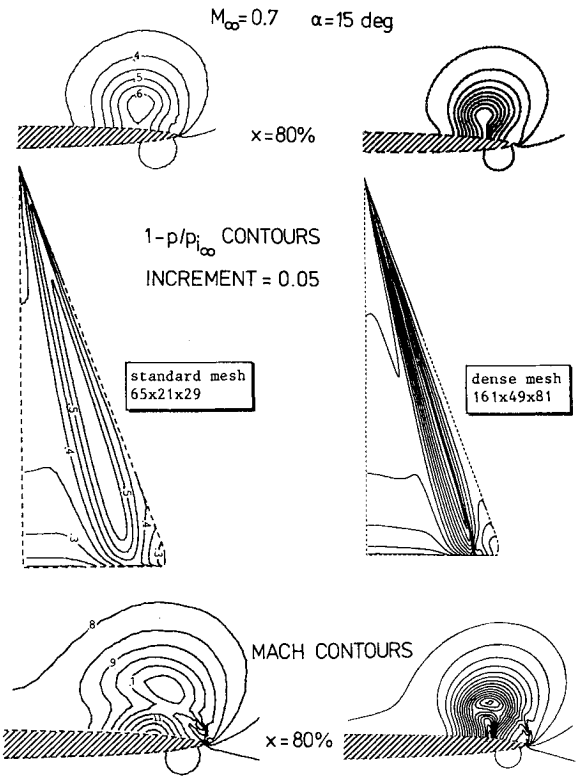


**Fig. 3 Comparison of isobars $1\text{-}p/p_{i_\infty}$ and iso-Mach contours computed with standard and dense meshes. $M_\infty = 0.70$, $\alpha = 15$ deg.**

chord, and 48 from the wing outward to the far field is presented in a variety of views in Figs. 3-5, including a blowup of the vorticity contours at the leading edge. The most striking feature (not seen in the standard-mesh solution but clearly visible here in the isobars, Mach number, and total pressure contours) is the small shock wave situated between the vortex and the upper surface of the wing just outboard of the vortex core. From observations of wind tunnel experiments, Vorropoulos and Wendt[9] have suggested the existence of just such a shock wave. In overall comparison with the standard-mesh solution, the suction peak under the vortex is markedly stronger and produces the shock wave, The smearing of vorticity across the vortex sheet at the leading edge is significantly reduced, and the total pressure losses are confined to a tighter region centered on the core of the vortex. On the upper surface of the wing the losses in the dense-mesh solution occur only across the shock. In the wake the interaction of the leading- and trailing-edge vortices also is represented better on the dense mesh.

A similar set of plots (Fig. 6) display selected views of iso-Mach contours of the solution computed for $M_\infty = 1.5$ and $\alpha = 15$ deg on a mesh of 192 cells around the semispan, 96 on the chord, and 56 from the wing outward to the far field. The variation in pressure throughout this supersonic flowfield is not very great but its minimum is very near vacuum. The coalescing of the Mach contours indicates the presence of a small shock wave intersecting the coiling vortex sheet just inboard of and above the core of the vortex. This feature of the flowfield is consistent with the experimental findings of Miller and Wood (see Ref. 10, Fig. 12). Furthermore, the constant Mach number contours of the dense-mesh solution on the upper surface of the wing show at least two distinct shock waves between the suction peak and leading edge, forming a complex system of shocks and expansion waves reflected back and forth across a narrow band that stretches from the apex to the trailing edge. Such phenomena should be expected because the flow, which is supersonic, has to turn abruptly where the vortex sheet leaves the leading edge. Accompanying these phenomena are heavy losses in total pressure.

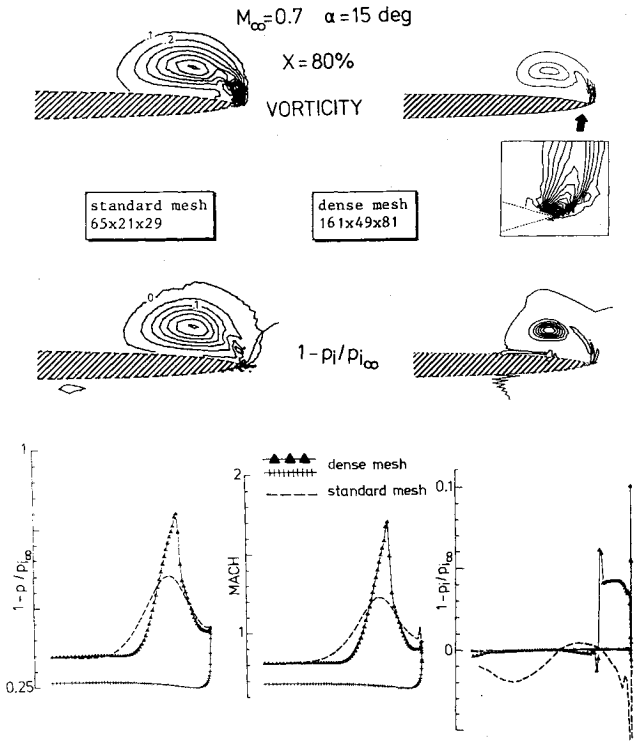


**Fig. 4 Contours of constant vorticity magnitude and total pressure $1\text{-}p_i/p_{i_\infty}$ computed with standard and dense meshes compared in the $x/c = 0.80$ surface. $M_\infty = 0.7$, $\alpha = 15$ deg.**

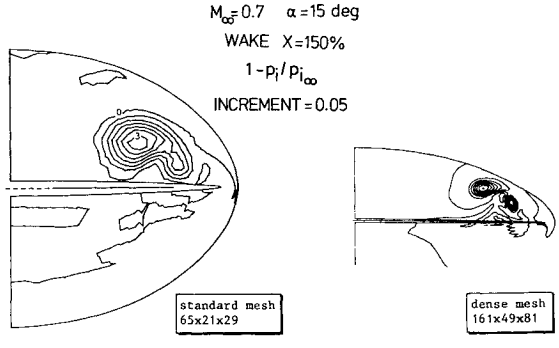


**Fig. 5 Total pressure contours $1\text{-}p_i/p_{i_\infty}$ computed with standard and dense meshes compared in the wake $x/c = 1.50$. $M_\infty = 0.7$, $\alpha = 15$ deg.**

## Total Pressure Loss

The loss in total pressure or, equivalently, an increase in entropy, is a puzzling question, particularly when no shock waves are present. At present there is no completely satisfying answer. Two points of view are maintainable: the observed loss in total pressure is purely a numerical artifact of the solution procedure and the resemblance to measurements in wind tunnels is strictly fortuitous, or it is the numerical approximation to a real physical feature of inviscid rotational flow. To substantiate the latter, one must describe the entropy-producing mechanism. Perhaps the analysis of the present results for the Dillner wing may provide some clues.

In general, the loss in total pressure is greater for the supersonic case than for the subsonic case, no doubt because of the nature of supersonic flow and the preponderance of shock waves. Therefore, it would be easier to recognize spurious losses in the subsonic case where shocks are less abundant. The comparison of standard and dense-mesh solutions, without and with a shock wave, respectively, might suggest that the small shock under the vortex is the cause of the loss of total pressure in the core. But the loss is only about 4% across

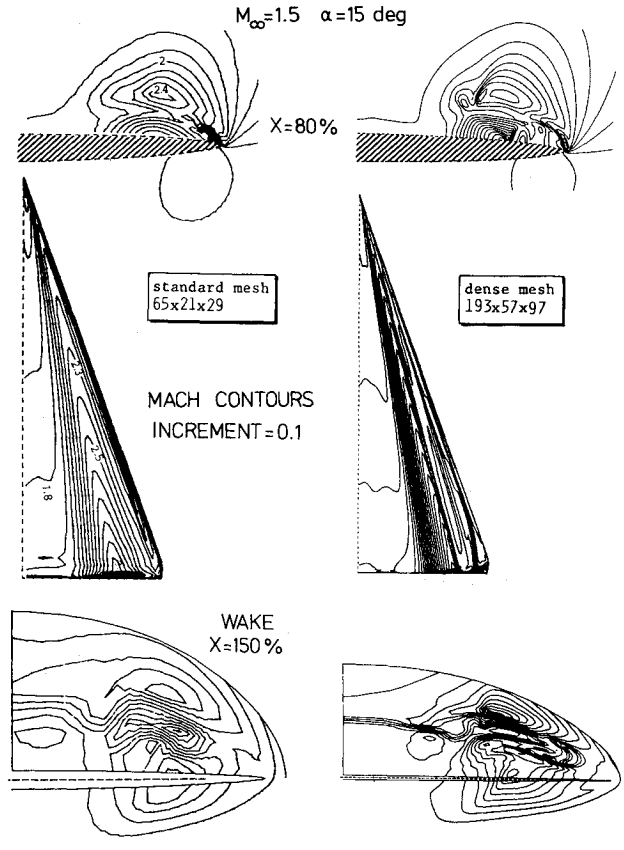


**Fig. 6 Comparison of standard- and dense-mesh iso-Mach contours. $M_\infty = 1.5$, $\alpha = 15$ deg.**

this shock but nearly 40% in the core of the vortex (see Fig. 4). Thus, there must be an additional contribution, which appears insensitive to mesh density since both solutions show about the same level of loss in the core (40%).

Both the standard- and dense-mesh solutions exhibit violent oscillations in the total pressure across a small region centered on the leading edge, which may be a numerical reaction to the capturing of the vortex sheet that is being shed there, or may indicate the presence in the real flow of a centered expansion fan imbedded very locally at the leading edge. If the latter is correct, the scale of the fan is smaller than this mesh, and even more refined calculations are needed to verify its existence. It is quite obvious, however, that even the slightest smearing of the velocity (or density) profile across the vortex sheet implies a loss in total pressure. Furthermore, the loss is greatest at that point of the profile that equals the average of the velocity vectors on each side of the sheet. Any losses created at the vortex sheet are then swept into the core. Although the breadth of the smeared layer may vary with mesh density (about seven mesh cells in each case), this may explain why the loss in the core does not vary in the same way.

The effect of a loss in total pressure is best seen in the Mach number distribution, but is hardly noticeable in the static pressure. A close inspection of these two properties (Fig. 7) reveals that the minimum static pressure in the core of the vortex does not coincide with either of the two local maxima in Mach number, but lies between them. The Mach number contours (Fig. 8) in a surface slicing streamwise through the core of the vortex provide a simple interpretation. The very pronounced zig-zag pattern in the iso-Mach contours across a relatively thin region strongly suggests the presence of a vortical layer that appears to originate at the apex of the wing. It is known that the conical singularity in the flow at the apex of the wing may produce an entropy gradient, therefore, it is tempting to speculate that the layer observed in Fig. 8 is a tube

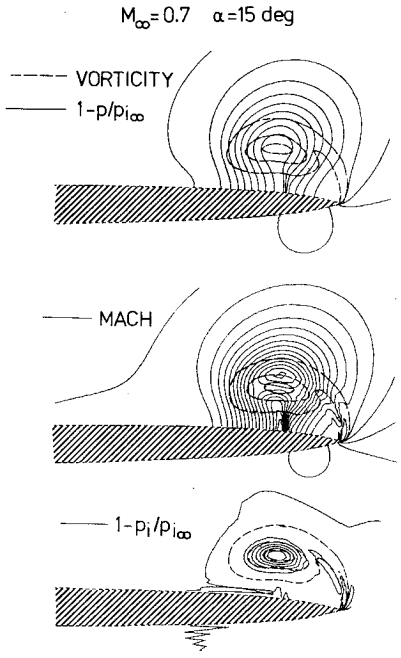


**Fig. 7 Variation of pressure, Mach number, and total pressure with vorticity in the 80% chord station. Dillner delta wing; $M_\infty = 0.7$, $\alpha = 15$ deg.**

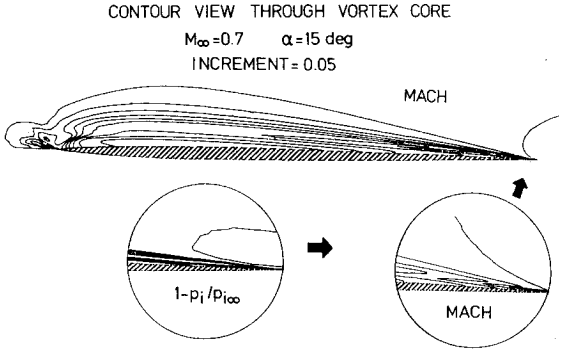


**Fig. 8 Iso-Mach contours in a mesh surface cutting through the axis of the vortex together with detail views at the apex. Dillner delta wing; $M_\infty = 0.7$, $\alpha = 15$ deg.**

of fluid that has gone through an entropy-producing process in the flow singularity at the apex. The Dillner wing is not conical but, at least locally at the apex, the flow might be expected to behave like a conical singularity. It seems unlikely, however, that the amount of entropy seen in the core could originate in this singularity. It more probably is due to the numerical error encountered when trying to integrate the Euler equations through a singular point. Figure 8 indicates the very large entropy gradients in a blowup view of the total pressure contours at the apex.

It seems virtually impossible to obtain an accurate solution at this singular point even with a much finer mesh because there is no length scale locally at the apex. Fortunately, this lack of resolution at the apex does not have a large effect on the overall large-scale flow features. The vortex does develop over the first three or four mesh surfaces in the stream direction for both the standard and dense meshes, presumably because of the overall flow conditions. Mesh refinement merely confines the region of inaccuracy due to the singularity to a smaller region of the flowfield.

## Concluding Remarks

The comparison of standard- and dense-mesh solutions to the Euler equations for vortex flow separating from the leading edge of the Dillner wing demonstrates that the creation of the vortex is not sensitive to the size of the mesh. A dense mesh, however, is necessary to resolve the rich structure of rotational flow interacting with shock waves, and to minimize diffusing of the captured vortex sheets. The size of the loss in total pressure seems to be invariant with the grid size, and appears to result from a singularity in the solution. The true singular solution is not resolved accurately, but is smeared over three to four mesh surfaces at the apex. Better resolution of this local flow feature does not seem essential for the creation of a realistic vortex flow.

## Acknowledgments

The author is grateful to Control Data Corporation for its interest in and support of this work, especially to Charles Purcell, who invited the author to Minneapolis, and Michael Hodous, who devoted many hours to help produce the solutions contained herein.

## References

[1] *Modelling and Computing: Aerodynamics of Vortical-Type Flow in Three Dimensions*, AGARD CP-342, Paris, 1983.

[2] *Test Cases for Steady Inviscid Transonic and Supersonic Flows*, Fluid Dynamics Panel Working Group 07, AGARD Pub., in preparation, 1985.

[3] Rizzi, A. W. and Bailey, H-E., "Finite Volume Solution of the Euler Equations for Steady Three-Dimensional Transonic Flow," Proceedings of the 5th *International Conference on Numerical Methods in Fluid Dynamics*, edited by A. I. van der Vooren and P. J. Zandbergen, *Lecture Notes in Physics*, Vol. 59 Springer Verlag, Berlin 1976, pp. 347-357.

[4] Rizzi, A. W. and Eriksson, L. E., "Computation of Flow Around Wings Based on the Euler Equations," *Journal Fluid Mechanics*, Vol. 148, Nov. 1984, pp. 45-71.

[5] Eriksson, L-E. and Rizzi, A., "Computer-Aided Analysis of the Convergence to Steady State of a Discrete Approximation to the Euler Equations," *Journal Computational Physics*, Vol. 57, No. 1, Jan. 1985, pp. 90-128.

[6] Eriksson, L-E., "Transfinite Mesh Generation and Computer-Aided Analysis of Mesh Effects," Doctoral Dissertation, Uppsala Univ., Uppsala, Sweden March 1984.

[7] Rizzi, A., "Vector Coding the Finite-Volume Procedure for the CYBER 205," *Lecture Series Notes 1983-84,* von Kármán Institute, Brussels, Belgium, 1983.

[8] Eriksson, L-E., "Generation of Boundary-Conforming Grids around Wing-Body Configurations using Transfinite Interpolation," *AIAA Journal* Vol. 20, Oct. 1982, pp. 1313-1320.

[9] Vorropoulos, G. and Wendt, J. F., "Laser Velocimetry Study of Compressibility Effects on the Flow Field of a Delta Wing," AGARD-CP-342, 1983.

[10] Miller, D. S. and Wood, R. M., "An Investigation of Wing Leading-Edge Vortices at Supersonic Speeds," AIAA Paper 83-1816, 1983.